Auxiliary Rapid Identification of Pathogenic and Antagonistic Microorganisms for Coptis Chinensis Root Rot by High-throughput Sequencing

Hailang Liao
Chengdu University of Traditional Chinese Medicine
Ling Huang
Chengdu University of Traditional Chinese Medicine
Na Li
Chengdu University of Traditional Chinese Medicine
Wenjia Ke
Chengdu University of Traditional Chinese Medicine
Yiqing Xiang
Chengdu University of Traditional Chinese Medicine
Yuntong Ma (mayuntong@cdutcm.edu.cn)
Chengdu University of Traditional Chinese Medicine

Research Article

Keywords: Root rot, C. Chinensis, Coptis root , pathogens , rhizosphere microbial community composition

Posted Date: January 5th, 2021

DOI: https://doi.org/10.21203/rs.3.rs-136612/v1

Abstract

Root rot reduced the yield and medical quality of *C. Chinensis*. Previous studies of *Coptis* root rot focused on the identification of pathogens and the rhizosphere microbial community composition. In order to provide more evidence for preventing this disease, the present study was to identify the pathogenic and antagonistic microorganisms based on a high-throughput sequencing technique. The healthy and diseased *C. chinensis* in the endosphere and rhizosphere from the same field were collected to investigating the differences in microbiome composition and function. The results showed that the composition and function of microbes were different. The animal pathogen, soil saprotroph, plant saprotroph, and wood saprotroph in the endosphere of the diseased *C. chinensis* were higher than the healthy endosphere, which was dominated by Phaeosphaeriaceae, *Cladorrhinum*, *Fusarium*, *Exophiala*, and Melanommataceae. *Fusarium*, *Volutella*, *Cladorhinum*, *Cylindrocarpon*, and *Exophiala* were significantly enriched in the endosphere of diseased plants. Co-occurrence network analysis showed that *Bacillus* were negatively correlated with *Fusarium*, *Volutella*, and *Cylindrocarpon*, indicating that they may be antagonistic microorganisms. To verify the sequencing results, *F. solani* and *F. avenaceum* have been isolated and verified as pathogens, and 14 *Bacillus* bacteria have been isolated, which displayed an apparent suppression effect against the two pathogens on PDA medium and detached root. The strategy of high-throughput sequencing has the potential for the comprehensive identification of pathogenic and antagonistic microorganisms for plant disease. These results lay the foundation for future studies on mitigating or preventing root rot damage to *C. chinensis*.

Introduction

COPTIDIS RHIZOMA (HuangLian) is a commonly used medicinal material in China, which derived from dry rhizomes of *Coptis chinensis* French., *C. deltoidea* Y. Cheng et Hsiao or *C. teeta* Wall. Due to the excessive mining of medicinal materials, the wild resources of COPTIDIS RHIZOMA have been exhausted. Currently, the demand for *Coptis* medicinal materials have risen sharply. As a result, the cultivation of *C. chinensis* has been the main source of this medicinal materials. However, *C. chinensis* has been planted in large areas with high-density in different regions, and the abuse of chemical fertilizers and pesticides has led to the diseases frequently occurrence in cultivated *Coptis* plants, mainly manifested by the high incidence of soil-borne diseases root rot.

According to the previous survey [1,2], the annual incidence of *Coptis* root rot in Shizhu, the largest production area of *C. chinensis* in China, is 10–20%, and the incidence in areas with severe disease is 60–90%, and even no harvest. When the root rot of *Coptis* plant occurs, the leaves of infected plants show wilt, necrotic lesions, drying, and death. The fibrous roots and rhizomes exhibited brown discoloration and progressive necrosis that caused mortality of the infected plants. *Fusarium solani* had first reported as the pathogen causing *C. chinensis* root rot [3], which was confirmed by Chen Shanshan et al. [4]. Recently, new *Fusarium* fungi have been reported as pathogens of *Coptis* root rot, mainly including *F. carminascens* [5], *F. oxysporum* [6], *F. tricinctum* [6], *F. avenaceum* [7]. But many obligate intracellular

pathogens do not grow in pure culture and never form reproductive structures, which render their detection and identification difficult. Rapid and accurate identification of pathogenic microorganisms is essential for detection and employment of appropriate mitigation measures

To date, there are also no effective prevention and control measures for *Coptis* root rot. Farmers generally adopt measures such as pulling out diseased plants, replacing soil, and irrigating potassium permanganate, but this effect is not obvious [2]. Research and development of new *Coptis* root rot prevention methods are imminent. In recent years, the use of antagonistic microorganisms as a biocontrol agent is attracting special attention, because it is a method of plant disease management with minimal impact on the environment [8–12]. In nature, there are various microorganisms in the growth environment of plants, and attaching to the surface and inside. These microorganism groups are collectively referred to as the plant microbiome, which can promote plant growth, inhibit disease occurrence and regulate plant microecological structure [13,14], and becoming an important determinant of plant health and growth [15,16]. The interspecies interaction of the plant microbiome increases the host's barrier against external pathogen colonization, thereby playing an important role in protecting the host's health [17,18]. Inoculation of native bacteria can significantly reduce the incidence of field diseases without affecting plant growth[19]. Root-related bacteria of healthy plants can affect the abundance and diversity of root filamentous eukaryotic microorganisms, thereby protecting the host from diseases caused by fungi and oomycetes[20].

High-throughput sequencing technology is a powerful tool to reveal the flora of plant diseases. It can detect plant pathogenic microorganisms and discover beneficial microorganisms that may inhibit plant pathogens and promote host growth, therefore providing possible solutions for plant pathogen infection and prevention [21–26]. Liu et al. [21] used 16S rRNA and ITS sequencing to identify the endophytic and rhizosphere microbiomes involved in ginseng rust roots. Ou et al. [24] used Illumina metabarcoding to trace changes in microbiome composition upon pathogens invasion over time, to investigate the expected changes in the microbiome between conductive and suppressive soil upon pathogen invasion, and to identify potential microbial agents that induce soil suppressiveness against *Fusarium* wilt disease.

Compared with previous studies, not only the rhizosphere, but also the endosphere microbial differences between healthy and diseased plants have been compared by amplicon sequencing. More importantly, we compared the differences between microbial composition and function, looked for indicator microorganisms, and constructed a microbial network to infer the interaction between microorganisms. In order to verify the reliability of evaluation method, the pathogen and beneficial microorganism have been isolated, identified, and functionally verified. This study not only helps the clarification of the fundamental cause of root rot, but also benefit the discovery of antagonistic microorganisms for the *Coptis* root rot prevention or control.

Result

Sequencing Data and OTU Clustering

After using high-throughput sequencing technology to remove low-quality, barcode and primer sequences, we finally got 1,369,013 valid 16S sequences for 12 samples subsequent analysis. The sequence lengths of valid sequences are distributed between 302 and 476 nt, where N50 > 443nt, N90 > 441nt. Then, the host chloroplast gene, mitochondrial gene, and the total number of tags do not exceed 5 sequences has been removed. The four groups produced a total of 10,989 OUTs, of which the CcGJ group, CcZJ group, CcGN group, and CcZN group contained OTU numbers are 3805, 3060, 3315, and 1768, respectively. The number of OUTs unique to the CcGJ group, CcZJ group, CcGN group, and CcZN group is 1585, 1239, 1123, and 369, respectively. Principal component analysis (PCA) showed that the CcGJ group and the CcGN group were relatively similar, and the differences among others were larger. It means that the rhizosphere of the diseased *C. chinensis* has a similar bacterial composition. The detailed results are shown in Table S1-S3 and Fig. 1A, C.

There were 2,041,477 valid ITS sequences used for subsequent analysis. The valid sequence lengths ranged from 204 to 399 nt, among which N50 > 340nt, N90 > 327nt. The host ITS2 gene and the total number of tags not more than 5 sequences were removed, 1,496 OTUs were generated. Among them, CcGJ group, CcZJ group, CcGN group and CcZN group contain 808, 934, 302, and 266 OTUs, respectively. The number of OUTs unique to CcGJ group, CcZJ group, CcGN group and CcZN group is 391, 508, 52, and 8, respectively. PCA analysis found that the CcGJ group and the CcZJ group were similar, and other differences were greater, indicating that the rhizosphere of the diseased and the healthy plants had a similar fungal composition. The detailed results are shown in Table S4-S6, Fig. 1B, D.

Composition of and Environmental Influence on the Coptis Roots Microbial Community

Shannon index (Figure S1) showed that there were significant differences in the richness and uniformity of bacterial OUT levels in the endosphere of diseased and healthy plants, and there were significant differences in the richness and uniformity of OUT levels of rhizosphere fungi between diseased and healthy plants.

β-diversity analysis showed that the root microbiome of *C. chinensis* was affected by disease and niche. In this study, Bray-Curtis distance among samples was analyzed by principal co-ordinate analysis (PcoA) and non-metric multi-dimensional scaling (NMDS) (Figure S2). The results were displayed on the first principal axis (Pco1/MDS1), and the root microbiome of *C. chinensis* was divided into two clusters according to whether it is diseased or not, indicating that the disease will cause drastic changes in the root microbiome of *C. chinensis*. On the second axis, the microbiome was divided into two clusters within the rhizosphere, which indicated that different ecological niches had a great influence on the root microorganisms of *C. chinensis*.

Fungal and Bacterial Taxa in Healthy and Diseased Coptis Roots

After the species annotation, a total of 40 bacterial phyla were identified. The top 10 species in abundance are shown in Figure S3. From the figure, the community composition and structure of the four groups are significantly different. Compared with healthy plants (CcZJ and CcZN groups), the relative abundance of Gemmatimonadetes and Parcubacteria bacteria in the endosphere of diseased plants (CcGJ and CcGN groups) increased significantly; Bacteroidetes increased significantly, and the relative abundance of Acidobacteria and Chlamydiae bacteria decreased significantly in the endosphere.

A total of 6 fungal phyla were identified (Figure S4). The relative abundance of Ascomycota fungi in the rhizosphere of healthy and diseased plants is the highest (over 60%). Compared with healthy plants (CcZJ and CcZN group), Chytridiomycota in the endosphere was significantly reduced for the diseased plants (CcGJ and CcGN group). In the rhizosphere, Rozellomycota and Chytridiomycota were significantly reduced.

Functional Analysis of Microbial in Healthy and Diseased Coptis Roots

For fungal communities, Funguild is an efficient method for analyzing fungal community data sets [27]. FUNGuild was used to predict the nutrient and functional groups of fungal communities in the rhizosphere and endosphere of diseased and healthy *C. chinensis*. The results showed that it was divided into 3 nutrition pattern groups (The sequences identified as multiple nutritional patterns was repeated calculation), among which the saprotroph of diseased endosphere was significantly higher than that of healthy endosphere ($P = 0.01439$). These fungi might be an important factor leading to the pathogenesis of *C. chinensis* root rot. Further analysis of the functional groups of the fungal community in the rhizosphere of *C. chinensis* (Fig. 2) showed that the animal pathogens and the soil saprotroph in the endosphere of the diseased *C. chinensis* were significantly higher ($P \leq 0.01$) than healthy endosphere. Plant saprotroph and wood saprotroph were significantly ($0.01 < P \leq 0.05$) higher than those in the roots of healthy endosphere. The plant pathogens in the rhizosphere of diseased *C. chinensis* were significantly higher ($0.01 < P \leq 0.05$) in the rhizosphere of healthy *C. chinensis*. The top 5 fungi types with significant differences in relative abundance in the endosphere of diseased plants included Phaeosphaeriaceae, *Cladorrhinum*, *Fusarium*, *Exophiala*, and Melanommataceae. The top 5 fungal groups with significant differences in the rhizosphere of diseased plants were Phaeosphaeriaceae, *Clonostachys*, *Fusarium*, *Phialophora*, and Chaetothyriaceae. The groups with significant differences shared by Phaeosphaeriaceae and *Fusarium*.

Based on 16 s rRNA gene information for PICRUSt2 analysis [28], we predicted the functional potential of the subgenome of bacterial communities. The results showed that the related prediction pathways belonging to the "tissue system" and "human diseases" had been removed, and there was no significant difference in the function of the bacterial community predicted in the rhizosphere of healthy and diseased *C. chinensis*; But there were significant differences in the predicted bacterial community function within the endospheree (Fig. 3). A total of 18 paths (KEGG level2) were predicted in the roots of diseased *Coptis* plants, which were significantly higher than those of healthy plants.

Indicator Species Analysis

The R project “labdsv” package was used to calculate the indicator value of each group for species with abundance value > 0 and total proportion > 0.1% in each sample of the comparison groups. Cross-validation of the statistical test was used to obtain the *P*-value. It is displayed as a bubble chart, and the biomarker of each group can be found intuitively by the size of the bubble. *Fusarium*, *Volutella*, *Cladorhinum*, *Cylindrocarpon*, and *Exophiala* were significantly enriched in the endosphere of diseased *C. chinensis* (Fig. 4). As shown in Figure S5, many bacteria were significantly enriched in the endosphere of the diseased *C. chinensis*, such as *Flavobacterium*, *Sphingobium*, *Chryseobacterium*, and B*revundimonas*. *Bacillus Collimonas, Rhizobium, Aquincola, Acidicapsa, and Edaphobacter were* enriched in the endosphere of the healthy *C. chinensis.*

Co-occurrence Network Construction and Analysis

The microbial network in the endosphere of the diseased *C. chinensis* consists of 60 genera (from 13 phyla) and 578 edges (Fig. 5, CcGN). The top 10 abundance genera included *Fusarium*, *Flavobacterium*, *Pedobacter*, *Caucobacter*, *Paucibacter*, *Ferribacterium*, *Nannocystis*, *Hydrogenophaga*, *Sphingobium*, and *Sphingopyxis*. The microbial network within the endosphere of healthy *C. chinensis* consisted of 36 genera (from 14 phyla) and 208 edges (Fig. 5, CcZN). Compared with healthy *C. chinensis*, CcGN has a higher clustering coefficient (0.933), total nodes (60), exclusive nodes (35), total edges (578), exclusive edges (46), and a lower average path length (1.093). It showed that there was a tighter and more complex microbial interaction network in the endosphere of diseased plants. The rhizosphere microbial network of diseased *C. chinensis* consisted of 40 genera (from 13 phyla) and 190 edges (Figure S6, CcGJ). The rhizosphere microbial network of healthy *C. chinensis* consisted of 40 genera (from 13 phyla) and 372 edges (Figure S6, CcZJ). The rhizosphere microbial network of diseased *C. chinensis* had a higher diameter (3), a higher exclusive node (18), an average path length (1.265), but a lower density (0.244), total edges (190), and exclusive edges (170). It showed that the rhizosphere microbial interaction network of *C. chinensis* rhizosphere changed obviously after the disease. The complexity and the interaction were reduced.

Microbial Isolation and Functional Verification

Two distinct fungal isolates (H1, H2) were isolated and Koch’s postulates were conducted to verify the pathogenicity of individual isolates (Fig. 6). The isolates were identified using an internal transcribed spacer (ITS) and translation elongation factor 1α (EF-1α) rRNA molecular analysis and morphological characteristics. They were identified as *F. solani* and *F. avenaceum* (Figure S7).

Based on KOMODO & GROWREC recommended media, 14 *Bacillus* bacteria have been isolated, which produced obvious inhibition bands to the two pathogens on PDA medium and detached root (Fig. 7, Fig. 8). From the healthy endosphere, 14 *Bacillus* bacteria with antagonistic activity against root rot pathogens of *C. chinensis* were isolated from the endosphere of healthy *C. chinensis*. They were identified as *B. subtilis* (830-002,JM-003), *B. velezensis* (JM-001, JM-002, JM-005), *B. pseudomycoides*

(LB-016, LB-050, LB-070, LB-074, NA-012, NA-048, YEM-014), and *B. mycoides* (LB-013, LB-021) based on 16 s RNA molecular identification (Figure S8). On PDA medium and detached root, four kinds of *Bacillus* bacteria produced obvious inhibition bands to the two pathogens. This indicated that they had an obvious inhibitory effect on two root rot pathogens of *C. chinensis*.

Discussion

Previous studies on *C. chinensis* root rot are mostly based on culture-dependent methods to isolate and identify a variety of pathogens of the genus *Fusarium* [29–32]. There are also two studies using high-throughput sequencing technology to study the bacterial and fungal community diversity in the rhizosphere of *C. chinensis* [1,33]. It was found that the bacterial richness and diversity of the rhizosphere significantly decreased, and the significant increase in the abundance of *Fusarium* was the main reason for the occurrence of root rot. However, Koch's postulates believe that pathogen comes from the inside of the host. It can be isolated and cultured from the host, and those pathogenic microorganisms can reinject the host and cause the host to have the same symptoms. The same pathogen can be isolated from the symptom site again. Therefore, the real pathogenic microorganisms must be found in the endosphere. Based on the previous studies, we have increased the research on microorganisms in the endosphere. Preliminary understanding of the microbial composition and function in the endosphere and rhizosphere of *C. chinensis*, and explore the possible pathogenic microorganisms of *C. chinensis* root rot and the beneficial microorganisms that can be used for disease control.

The microbial diversity showed that the α-diversity of the rhizosphere fungi of the diseased plants was significantly higher than that of the healthy plants, and the α-diversity of the bacteria in the endosphere of the diseased plants was significantly higher than that of the healthy plants. The pathogens destroyed the plant tissue and entered into the rhizosphere soil, which led to the increase of the α-diversity of rhizosphere fungi. The diseased tissue may recruit more bacteria to resist the infection of pathogens, which lead to the increase of bacterial α-diversity in the endosphere of diseased plants. PCoA and NMDS analysis can proved this, which showed that the root microbiome of *C. chinensis* was significantly affected by disease and niche.

FunGuild was used to predict the function of fungi in the endosphere and rhizosphere of *C. chinensis*. It was found that the saprotroph type in the endosphere of diseased plants was significantly higher than that in the endosphere of the healthy plant. Further analysis of the functional groups for the fungal community revealed that the animal pathogens, soil saprotroph, plant saprotroph, and wood saprotroph were significantly higher than that in the endosphere of healthy plants. The plant pathogens in the rhizosphere of diseased plants were significantly higher than that of healthy plants. Therefore, these fungi may be the main pathogens of *C. chinensis* root rot. PICRIUSt2 predicted the function of bacteria and found that the bacteria in the endosphere of the diseased plant could obtain more nutrient resources than healthy plants, and the metabolism was stronger. They had obvious interactions and tended to adapt to changes in the environment. These results indicated that the root system of *C. chinensis* might be recruiting more microorganisms to fight the pathogenic bacteria of root rot.

Indicator species analysis found that the endosphere of the diseased plants was significantly enriched in *Fusarium*, *Volutella*, *Cladorhinum*, *Cylindrocarpon*, *Exophiala*, and *Flavobacterium*. According to the literature reports, *Fusarium* are one of the most important groups of plant pathogenic fungi, which causes a series of diseases on a variety of crops and affects the diversity of crops in various climate regions around the world [34]. *Fusarium* are also the main culprit of *Coptis* root rot reported in the literature [3–7, 35,36]. *Volutella* are pathogens that cause Volutella blight in a variety of hosts [29,30,37]. *Cylindrocarpon* are the important pathogens that cause rust rot in ginseng and American ginseng [38]. Most of the studies on *Exophiala* are reported as the pathogens of animal and human diseases [39,40]. *Cladorrhinum* biological control fungi (*Cladorrhinum foecundissimumto*) can reduce viral diseases caused by *Rhizobia* and *Pythium*[31], and endophytic bacteria *Cladorrhinum foecundissimum* can prevent cotton root rot caused by *Rhizoctonia solani* [41]. Members of *Flavobacterium* can promote plant growth by producing auxin, gibberellin, and cytokinin [42,43]. Their powerful combination of extracellular enzymes is believed to be related to the degradation of bacteria, fungi, insects, and nematodes in the environment. They play an important role in plant defense [44]. Therefore, the pathogenic microorganisms of *C. chinensis* root rot are not only *Fusarium* fungi, but also other microorganisms that cause root rot or the accomplice of *Fusarium*, such as *Volutella*, *Exophiala*, and *Cylindrocarpon* fungi. At the same time, the diseased *C. chinensis* may recruit some microorganisms including *Cladorrhinum* and *Flavobacterium* to fight against pathogenic bacteria.

Poudel et al. [45] pointed out that the co-occurrence network analysis of plant microbial communities could provide a new perspective for strengthening disease management and identifying candidate microorganisms affecting plant health. The results showed that there were significant differences in the microbial symbiosis network in the endosphere and rhizosphere of healthy and diseased *C. chinensis*. Compared with the microbial network in the endosphere of healthy plants (CcZN), the microbial network in the endosphere of diseased plants (CcGN) had a tighter and more complex microbial interaction network. The ecological network is a standard method for describing and analyzing direct interactions among species. The network structure controls the stability of ecological communities [46], including their ability to be invaded by new species [47]. Through the microbial network, it was found that *Bacillus*, *Plantomyces*, *Rhizobium*, and *Roseiarcus* were all negatively correlated with *Fusariun*, *Volutella*, and *Cylindrocarpon* in the healthy endosphere. According to the literature reports, many *Bacillus* have been proven to be effective against a wide range of plant pathogens [48]. They have been reported as plant growth promoters, systemic resistance inducers, and produce a wide range of antibacterial compounds (lipopeptides, lipopeptides, Antibiotics, and enzymes) [49] and growth factors (space and nutrients) competitors [50]. Compounds with antifungal and bacterial activities can be isolated from *Planctomyces* bacteria [51,52]. *Rhizobium* has an antagonistic effect on fungi [53], as a biological control bacterium for plant root rot [54–56], and promotes host growth [57]. *Roseiarcus* are mycorrhiza helper bacteria (MHB) [58], which can spread to the root tips [59], promote the growth and colonization of mycorrhizas [60,61]. We believe that *Bacillus*, *Plantomyces*, *Rhizobium*, and *Roseiarcus* may be the key microorganisms to maintain the healthy growth of *C. chinensis*.

Considering the prevalence of *Fusarium* in root rot of *C. chinensis* and high relative abundance of *Bacillus* in healthy plants root, selective isolation and functional verification of Fusarium and Bacillus were carried out. *F. solani* and *F. avenaceum* have been isolated and verificated as the pathogen of *C. chinensis* root rot based on Koch's postulates. *F. solani* [3] and *F. avenaceum* [7] have been reported by some other articles as the pathogen of *C. chinensis*, which also able to prove the correctness of our conjecture. But we did not isolate any fungi belong to *Volutella*, *Exophiala*, and *Cylindrocarpon*, we can't tell whether they are also pathogenic of *coptis* root rot or not, because this need more isolation methods to culture them. From the healthy endosphere, 14 Bacillus *bacteria* with antagonistic activity against root rot pathogens of *C. chinensis* were isolated. They were identified as *B. subtilis*, *B. velezensis*, *B. pseudomycoides*, and *B. mycoides* by 16 s RNA molecular identification. The accuracy of our conjecture on antagonistic microorganisms of *C. chinensis* root rot was partly proved. The strategy of high-throughput sequencing has the potential for comprehensive identification of pathogenic and antagonistic microorganisms for plant disease.

Methods

Experimental Design and Sampling

Collection and Processing of Experimental Materials

The healthy and root rot diseased of *C. chinensis* roots from the same field were taken from the *C. chinensis* cultivation bases of Wawushan Pharmaceutical Co., Ltd. in Hongya County (Group 2, Heishan Village, Gaomiao Town, Hongya County, Meishan City, Sichuan Province,China 29°29'10.91" N 103°9'39.9" E) in November 2018. Five healthy or diseased plants were mixed as a duplicate sample. The healthy and diseased plants were repeated 3 times, respectively, packed in a sterile plastic bag and put into a fresh-keeping box with ice packs before arriving in the laboratory for immediate disposal.

The loose soil around the roots of *C. chinensis* was shaken off until only soil adhered to the root surface remained, and the fibrous roots were cut and placed in a sterile 50 mL centrifuge tube. The rhizosphere soil on fibrous roots were released by sonication using a 30-s pulse–30-s off-cycle, and repeated 4 times. The suspension was centrifuged with the supernatant discarded for the rhizosphere soil. The fibrous roots samples described above were surface sterilized by consecutive immersion for 30 s in 75% ethanol, and 10 min in 2% sodium hypochlorite, followed by 4 rinses in sterile distilled water. The rhizosphere soil and the fibrous were quickly frozen by liquid nitrogen and stored in a refrigerator at -80 °C until required for DNA extraction.

DNA Extraction and PCR Amplification

Microbial DNA was extracted using the HiPure Soil DNA Kits (Magen, Guangzhou, China) according to the manufacturer's protocols. The 16S rDNA V3-V4 region of the ribosomal RNA gene were amplified by PCR

using primers 341F: CCTACGGGNGGCWGCAG; 806R: GGACTACHVGGGTATCTAAT [62]. The fungal ITS2 region was amplified using the primers ITS3_KYO2: GATGAAGAACGYAGYRAA; ITS4: TCCTCCGCTTATTGATATGC [63]. PCR reactions were performed in triplicate 50 μL mixture containing 5 μL of 10 × KOD Buffer, 5 μL of 2 mM dNTPs, 3 μL of 25 mM $MgSO_4$, 1.5 μL of each primer (10 μM), 1 μL of KOD Polymerase, and 100 ng of template DNA. The reaction conditions were as follows: 94 °C for 2 min, followed by 30 cycles at 98℃ for 10 s, 62℃ for 30 s, and 68℃ for 30 s and a final extension at 68 °C for 5 min.

Illumina Hiseq 2500 Sequencing

Amplicons were extracted from 2% agarose gels and purified using the AxyPrep DNA Gel Extraction Kit (Axygen Biosciences, Union City, CA, U.S.) according to the manufacturer's instructions and quantified using ABI StepOnePlus Real-Time PCR System (Life Technologies, Foster City, USA). Purified amplicons were pooled in equimolar and paired-end sequenced (2 × 250) on an Illumina platform according to the standard protocols[64]. The raw reads were deposited into the NCBI Sequence Read Archive (SRA) database (Accession Number: SRP286246).

Isolation and Characterization of the Pathogen

In November 2018, 33 diseased roots from the same field with high-throughput sequencing samples were collected from Sichuan (29°29'10.91" N,103°9'39.9" E), and small samples (0.5 cm in length) were cut from the border between diseased and healthy tissue, successively sterilized with 75% ethanol and 2% sodium hypochlorite, rinsed 3 times in sterilized water, dried on sterilized filter paper, and transferred onto PDA, and incubated at 25 °C for 7 days in the dark. Two distinct fungal isolates (H1, H2) were isolated and Koch's postulates were conducted to verify the pathogenicity of individual isolates. The isolates were identified using an internal transcribed spacer (ITS) and translation elongation factor 1α (EF-1α) rRNA molecular analysis and morphological characteristics.

Isolation, Identification, and Activity of Antagonistic Bacteria

The antagonistic microorganisms were isolated using the media that KOMODO & GROWREC (http://komodo.modelseed.org/default.htm) recommended based on 16 s rRNA or the genus name. The antagonistic interaction between antagonistic microorganisms and pathogen was studied on PDA media by the dual culture method. The PDA medium without the antagonistic bacteria was used as the control. The activity isolates were identified based on their 16S rRNA molecular analysis using PAUP * 4.0 Beta 10 with the maximum parsimony method. Then the identified bacteria were used to measure the antagonistic ability on the detached root, with the sterile water used as blank control. The lower 1/4 of

fibrous roots were inoculated with spores of two kinds of pathogens (2.1×10^7 CFU/mL, 100 μL), and the upper 1/4 of morphology was inoculated with a corresponding *bacillus* (OD_{600} = 1, 100 μL). After 7 days of moistening culture, the incidence of detached roots was observed.

Data Analysis

16S and ITS2 rRNA Gene Bioinformatics Process

The Illumina Miseq platform was used to identify the questionable sequence; USEARCH and VEARCH 2.14 were used to merge the double-ended sequences; The primers and quality control were removed. The sequences were de-redundant and OTU was generated according to 97% similarity, and the effective sequence of each sample was obtained. We called USEARCH for 16S rDNA V3-V4 region sequence based on Silva (Version 138) [65,66], ITS2 region sequence based on UNITE (Version 04.02.2020) [67]. After removing chimera sequences and annotate species, we removed chloroplasts and mitochondria, host ITS2 sequence, and tag number should not exceed 5 sequences in total.

Diversity and Statistical Analysis

The Shannon α-diversity index was calculated in QIIME (version 1.9.1). R project “ggplot2” package [68] (version 2.2.1) was used to draw a histogram. The Shannon index between the two groups was analyzed by Welch's T-test [32]. Muscle [69] (version 3.8.31) was used to sequence alignment, and FastTree [70] (version 2.1) was used to construct a phylogenetic tree, and then we performed Bray-Curtis in the R project “Vegan” package [32] (version 2.3.5). Multivariate statistical analysis of PCoA and NMDS of Bray-Curtis distance, and plotted in the “ggplot2” package [68] with Welch's T-test.

Analysis of Functional Differences

PICRUSt2 [28] was used to predict the functional genes of the bacterial community, and FunGuild [27] was used to predict the fungal community function. The statistical analysis of STAMP software [71] was used to detect the significant difference in the abundance of functional genes/paths corresponding to the healthy group and the diseased group. Apply Welch’s T-test ($P < 0.05$) and Benjamini-Hochberg's false discovery rate (FDR) multiple test correction to generate extended error bar graphs or draw statistical stacked shock graphs. The R project “ggalluvial” package (Version 0.12.2) was used to draw the fungal function stacked shock map.

Indicator Species Analysis

The R language “labdsv” package was used to calculate the indicator value of each group of species with abundance value > 0 and total proportion > 0.1% in each sample of the comparison group. Cross-

validation for statistical tests was used to obtain the P-value. It is displayed as a bubble chart, and the biomarker of each group can be found intuitively by the size of the bubble.

Species Network Construction and Key Taxa Analysis

The genera with relative abundance greater than 1% identified in the rhizosphere and endosphere of healthy and diseased *Coptis* plants were selected. We merged each group of fungal and bacteria, used the CoNet plug-in [72] of Cytoscape 3.80 software [73] for network analysis. “Pearson correlation” and “Spearman correlation” was specified as 0.7 to construct a microbial interaction network. A permutation test was performed to obtain p-value, and filter out invalid edges with the p-value greater than 0.01. In order to calculate the statistical significance of co-occurrence and mutual exclusion, we calculated the edge-specific permutation and bootstrap score distribution for 1000 iterations to obtain the final network [74] and visualized the network through Cytoscape 3.80.

Declarations

Acknowledgments

This work was supported by Sichuan Science and Technology Support Program (2014SZ0156). The authors also thank the National Wild Plant Germplasm Resources Infrastructure for its support.

Author Contributions

H.L. and L.H. co-designed and conducted the experiment, performed bioinformatics and statistics, analyzed, and interpreted the data, and wrote the manuscript. N.L., W.K., and Y.X. conducted the experiment and wrote the manuscript. Y.M. designed the experiment, contributed to data interpretation and manuscript writing, and obtained financial support. All authors revised and approved the final version of the manuscript.

Competing interests

The authors declare no competing interests.

References

1. Xuhong, S., Yu, W., Longyun, L. & Jun, T. Research on bacteria microecology in root rot rhizosphere soil of Coptis chinensis produced in Shizhu city. *China Journal of Chinese Materia Medica.* **42**, 1304–1311 https://doi.org/10.19540/j.cnki.cjcmm.20170222.012 (2017).

2. Fujun, Y., Wei, Z. & Xianyou, Q. Investigation of the main diseases of Coptidis and control strategy. *Plant Doctor* **22**, 21–23, https://doi.org/CNKI:SUN:CQZY.0.2010-01-062 (2009).
3. Luo, X. M. *et al.* First Report of Fusarium solani Causing Root Rot on Coptis chinensis in Southwestern China. *Plant Dis.* **98**, 1273 https://doi.org/10.1094/PDIS-02-14-0164-PDN (2014).
4. Shanshan, C., Xiumei, L. & Xingyong, Y. Isolation and identification of Coptis chinensis root rot pathogen in Shizhu County, Chongqing City. *Journal of Plant Protection.* **45**, 1437–1438 https://doi.org/10.13802/j.cnki.zwbhxb.2018.2017154 (2018).
5. Huanhuan, C. *et al.* Identification and fungicide sensitivity of pathogen causing root rot of goldthread. *Journal of Plant Pathology.* **50**, 377–380 https://doi.org/10.13926/j.cnki.apps.000329 (2020).
6. Xiaoli, W., Yu, W., Fei, L., Daxia, C. & Longyun, L. Identification of Coptis chinensis root rot disease pathogenic Fusarium spp. fungi. *China Journal of Chinese Materia Medica.* **45**, 1323–1328 https://doi.org/10.19540/j.cnki.cjcmm.20200112.102 (2020).
7. Mei, P., Song, X., Zhu, Z. & Li, L. First Report of Root Rot Caused by Fusarium avenaceum on Coptis chinensis Franchet in Chongqing, China. *Plant Dis.* https://doi.org/10.1094/PDIS-05-20-1110-PDN (2020).
8. De Silva, N. I., Brooks, S., Lumyong, S. & Hyde, K. D. Use of endophytes as biocontrol agents. *Fungal Biology Reviews.* **33**, 133–148 https://doi.org/10.1016/j.fbr.2018.10.001 (2019).
9. Rojas, E. C. *et al.* Selection of fungal endophytes with biocontrol potential against Fusarium head blight in wheat. *Biol Control.* **144**, https://doi.org/10.1016/j.biocontrol.2020.104222 (2020).
10. Lecomte, C., Alabouvette, C., Edel-Hermann, V., Robert, F. & Steinberg, C. Biological control of ornamental plant diseases caused by Fusarium oxysporum: A review. *Biol Control.* **101**, 17–30 https://doi.org/10.1016/j.biocontrol.2016.06.004 (2016).
11. Vinayarani, G. & Prakash, H. S. Fungal endophytes of turmeric (Curcuma longa L.) and their biocontrol potential against pathogens Pythium aphanidermatum and Rhizoctonia solani. *World Journal of Microbiology and Biotechnology.* **34**, 49 https://doi.org/10.1007/s11274-018-2431-x (2018).
12. Syed, A., Rahman, S. F., Singh, E., Pieterse, C. M. J. & Schenk, P. M. Emerging microbial biocontrol strategies for plant pathogens. *Plant Sci.* **267**, 102–111 https://doi.org/10.1016/j.plantsci.2017.11.012 (2018).
13. Antoun, H. in Brenner's Encyclopedia of Genetics (eds Kelly Hughes & Stanley Maloy) 353–355 (Elsevier Science Publishing Co. Inc., 2013).
14. Muller, D. B., Vogel, C., Bai, Y. & Vorholt, J. A. The Plant Microbiota: Systems-Level Insights and Perspectives. *Annual Review of Genetics.* **50**, 211–234 https://doi.org/10.1146/annurev-genet-120215-034952 (2016).
15. Mendes, R. *et al.* Deciphering the rhizosphere microbiome for disease-suppressive bacteria. *Science.* **332**, 1097–1100 https://doi.org/10.1126/science.1203980 (2011).

16. Qu, Q. *et al.* Rhizosphere Microbiome Assembly and Its Impact on Plant Growth. *J. Agric. Food Chem.* **68**, 5024–5038 https://doi.org/10.1021/acs.jafc.0c00073 (2020).
17. Ramayo-Caldas, Y. *et al.* Phylogenetic network analysis applied to pig gut microbiota identifies an ecosystem structure linked with growth traits. *The ISME Journal.* **10**, 2973–2977 https://doi.org/10.1038/ismej.2016.77 (2016).
18. Xiong, J. *et al.* Changes in intestinal bacterial communities are closely associated with shrimp disease severity. *Appl. Microbiol. Biotechnol.* **99**, 6911–6919 https://doi.org/10.1007/s00253-015-6632-z (2015).
19. Santhanam, R. *et al.* Native root-associated bacteria rescue a plant from a sudden-wilt disease that emerged during continuous cropping. *Proc Natl Acad Sci U S A.* **112**, E5013–5020 https://doi.org/10.1073/pnas.1505765112 (2015).
20. Duran, P. *et al.* Microbial Interkingdom Interactions in Roots Promote Arabidopsis Survival. *Cell.* **175**, 973–983914 https://doi.org/10.1016/j.cell.2018.10.020 (2018).
21. Liu, D., Sun, H. & Ma, H. Deciphering Microbiome Related to Rusty Roots of Panax ginseng and Evaluation of Antagonists Against Pathogenic Ilyonectria. *Frontiers of Microbiology.* **10**, 1350 https://doi.org/10.3389/fmicb.2019.01350 (2019).
22. Tedersoo, L., Drenkhan, R., Anslan, S., Morales-Rodriguez, C. & Cleary, M. High-throughput identification and diagnostics of pathogens and pests: Overview and practical recommendations. *Molecular Ecology Resources.* **19**, 47–76 https://doi.org/10.1111/1755-0998.12959 (2019).
23. Pentimone, I., Colagiero, M., Rosso, L. C. & Ciancio, A. Omics applications: towards a sustainable protection of tomato. *Appl. Microbiol. Biotechnol.* https://doi.org/10.1007/s00253-020-10500-7 (2020).
24. Ou, Y. *et al.* Deciphering Underlying Drivers of Disease Suppressiveness Against Pathogenic Fusarium oxysporum. *Frontiers of Microbiology.* **10**, 2535 https://doi.org/10.3389/fmicb.2019.02535 (2019).
25. Meng, T., Wang, Q., Abbasi, P. & Ma, Y. Deciphering differences in the chemical and microbial characteristics of healthy and Fusarium wilt-infected watermelon rhizosphere soils. *Appl. Microbiol. Biotechnol.* **103**, 1497–1509 https://doi.org/10.1007/s00253-018-9564-6 (2019).
26. Jakuschkin, B. *et al.* Deciphering the Pathobiome: Intra- and Interkingdom Interactions Involving the Pathogen Erysiphe alphitoides. *Microb. Ecol.* **72**, 870–880 https://doi.org/10.1007/s00248-016-0777-x (2016).
27. Nguyen, N. H. *et al.* FUNGuild: An open annotation tool for parsing fungal community datasets by ecological guild. *Fungal Ecol.* **20**, 241–248 https://doi.org/10.1016/j.funeco.2015.06.006 (2016).
28. Douglas, G. M. *et al.* PICRUSt2: An improved and extensible approach for metagenome inference. *bioRxiv.* **672295**, https://doi.org/10.1101/672295 (2019).
29. Garibaldi, A., Bertetti, D., Ortu, G. & Gullino, M. L. First Report of Volutella Blight caused by Pseudonectria buxi on Japanese Boxwood (Buxus microphylla) in Italy. *Plant Dis.* **100**, 1499 https://doi.org/10.1094/pdis-09-15-1027-pdn (2016).

30. Bai, Q., Xie, Y., Dong, R., Gao, J. & Li, Y. First Report of Volutella Blight on Pachysandra Caused by Volutella pachysandricola in China. *Plant Dis.* **96**, 584–584 https://doi.org/10.1094/pdis-11-11-0997 (2012).
31. Lewis, J. A. & Larkin, R. P. Formulation of the Biocontrol Fungus Cladorrhinum foecundissimumto Reduce Damping-Off Diseases Caused by Rhizoctonia solani and Pythium ultimum. *Biol Control.* **12**, 182–190 https://doi.org/10.1006/bcon.1998.0639 (1998).
32. Oksanen, J. *et al.* vegan: Community Ecology Package. https://github.com/vegandevs/vegan (2016).
33. Xuhong, S., Jun, T. & Long-yun, L. u, W. Y. & Xiao-li, W. Illumina high-throughput sequencing reveals fungal community composition and diversity in root rot of *Coptis chinensis* in rhizosphere soil *Chinese Traditional and Herbal Drugs* **49**, 5396–5403, https://doi.org/10.7501/j.issn.0253-2670.2018.22.026 (2018).
34. Summerell, B. A. Resolving Fusarium: Current Status of the Genus. *Annual Review of Phytopathology.* **57**, 323–339 https://doi.org/10.1146/annurev-phyto-082718-100204 (2019).
35. Xiaoli, W., Fei, L., Daxia, C., Yu, W. & Longyun, L. Diversity of culturable fungi isolated from the Coptis chinensis rot root in Shizhu city of Chongqing. *China Journal of Chinese Materia Medica.* 1–13 https://doi.org/10.19540/j.cnki.cjcmm.20190729.102 (2019).
36. Changyun, L. *et al.* Analysis of pathogenic factors of Coptis root rot and screening of control agents. *Plant Doctor.* **32**, 24–27 https://doi.org/10.13718/j.cnki.zwys.2019.04.005 (2019).
37. Wang, X., Li, Y. X., Dong, H. X., Jia, X. Z. & Zhang, X. Y. First Report of Volutella buxi Causing Volutella Blight on Buxus bodinieri in Central Plains China. *Plant Dis.* **101**, 1325 https://doi.org/10.1094/pdis-10-16-1487-pdn (2017).
38. Xuerui, Y. & Junfan, F. A. Summaryof Researches on Cylindrocarpon and Panax Root Rust- rot. *Journal of Shenyang Agricultural University.* **33**, 71–75 https://doi.org/10.3969/j.issn.1000-1700.2002.01.020 (2002).
39. Wen, Y. M., Rajendran, R. K., Lin, Y. F., Kirschner, R. & Hu, S. Onychomycosis Associated with Exophiala oligosperma in Taiwan. *Mycopathologia.* **181**, 83–88 https://doi.org/10.1007/s11046-015-9945-7 (2016).
40. de Hoog, G. S. *et al.* Waterborne Exophiala species causing disease in cold-blooded animals. *Persoonia.* **27**, 46–72 https://doi.org/10.3767/003158511X614258 (2011).
41. Gasoni, L. & de Gurfinkel, S. Biocontrol of Rhizoctonia solani by the endophytic fungus Cladorrhinum foecundissimum in cotton plants. *Australas Plant Path.* **38**, 389–391 https://doi.org/10.1071/AP09013 (2009).
42. Anbukkarasi, K., Hemalatha, T. & Chendrayan, K. Studies on phytohormone producing ability of indigenous endophytic bacteria isolated from tropical legume crops. *International Journal of Current Microbiology and Applied Sciences.* **2**, 127–136 https://doi.org/10.1002/chin.200352224 (2013).
43. Kolton, M., Erlacher, A., Berg, G. & Cytryn, E. in Microbial Models: From Environmental to Industrial Sustainability (ed Susana Castro-Sowinski) 189–207 (Springer Singapore, 2016).

44. Kolton, M., Frenkel, O., Elad, Y. & Cytryn, E. Potential role of Flavobacterial gliding-motility and type IX secretion system complex in root colonization and plant defense. *Mol Plant Microbe In.* **27**, 1005–1013 https://doi.org/10.1094/MPMI-03-14-0067-R (2014).
45. Poudel, R. *et al.* Microbiome Networks: A Systems Framework for Identifying Candidate Microbial Assemblages for Disease Management. *Phytopathology.* **106**, 1083–1096 https://doi.org/10.1094/PHYTO-02-16-0058-FI (2016).
46. Thébault, E. & Fontaine, C. Stability of Ecological Communities and the Architecture of Mutualistic and Trophic Networks. *Science.* **329**, 853–856 https://doi.org/10.1126/science.1188321 (2010).
47. Hui, C. *et al.* Defining invasiveness and invasibility in ecological networks. *Biol. Invasions.* **18**, 971–983 https://doi.org/10.1007/s10530-016-1076-7 (2016).
48. Shafi, J., Tian, H. & Ji, M. Bacillus species as versatile weapons for plant pathogens: a review. *Biotechnology & Biotechnological Equipment.* **31**, 446–459 https://doi.org/10.1080/13102818.2017.1286950 (2017).
49. Wang, G., Li, X. & Wang, Z. APD3: the antimicrobial peptide database as a tool for research and education. *Nucleic Acids Res.* **44**, D1087–1093 https://doi.org/10.1093/nar/gkv1278 (2016).
50. Fira, D., Dimkić, I., Berić, T., Lozo, J. & Stanković, S. Biological control of plant pathogens by Bacillus species. *Journal of Biotechnol.* **285**, 44–55 https://doi.org/10.1016/j.jbiotec.2018.07.044 (2018).
51. Graca, A. P., Calisto, R. & Lage, O. M. Planctomycetes as Novel Source of Bioactive Molecules. *Frontiers of Microbiology.* **7**, 1241 https://doi.org/10.3389/fmicb.2016.01241 (2016).
52. Wiegand, S., Jogler, M. & Jogler, C. On the maverick Planctomycetes. *FEMS Microbiology Reviews.* **42**, 739–760 https://doi.org/10.1093/femsre/fuy029 (2018).
53. Chao, W. L. Antagonistic activity of Rhizobium spp. against beneficial and plant pathogenic fungi. *Letters in Applied Microbiology.* **10**, 213–215 https://doi.org/10.1111/j.1472-765X.1990.tb01336.x (1990).
54. Sayeed Akhtar, M. & Siddiqui, Z. A. Biocontrol of a root-rot disease complex of chickpea by Glomus intraradices, Rhizobium sp. and Pseudomonas straita. *Crop Prot.* **27**, 410–417 https://doi.org/10.1016/j.cropro.2007.07.009 (2008).
55. Das, K., Prasanna, R. & Saxena, A. K. Rhizobia: a potential biocontrol agent for soilborne fungal pathogens. *Folia Microbiol.* **62**, 425–435 https://doi.org/10.1007/s12223-017-0513-z (2017).
56. Volpiano, C. G. *et al.* in Microbiome in Plant Health and Disease: Challenges and Opportunities (eds Vivek Kumar, Ram Prasad, Manoj Kumar, & Devendra K. Choudhary)315–336(Springer Singapore, 2019).
57. Siddiqui, Z. A., Baghel, G. & Akhtar, M. S. Biocontrol of Meloidogyne javanica by Rhizobium and plant growth-promoting rhizobacteria on lentil. *World Journal of Microbiology and Biotechnology.* **23**, 435–441 https://doi.org/10.1007/s11274-006-9244-z (2006).
58. Yu, F., Liang, J. F., Song, J., Wang, S. K. & Lu, J. K. Bacterial Community Selection of Russula griseocarnosa Mycosphere Soil. *Frontiers of Microbiology.* **11**, 347 https://doi.org/10.3389/fmicb.2020.00347 (2020).

59. Poole, E. J., Bending, G. D., Whipps, J. M. & Read, D. J. Bacteria associated with Pinus sylvestris–Lactarius rufus ectomycorrhizas and their effects on mycorrhiza formation in vitro. *New Phytol.* **151**, 743–751 https://doi.org/10.1046/j.0028-646x.2001.00219.x (2001).
60. Pent, M., Poldmaa, K. & Bahram, M. Bacterial communities in boreal forest mushrooms are shaped both by soil parameters and host identity. *Frontiers of Microbiology.* **8**, 836 https://doi.org/10.3389/fmicb.2017.00836 (2017).
61. Nguyen, N. H. & Bruns, T. D. The Microbiome of Pinus muricata Ectomycorrhizae: Community Assemblages, Fungal Species Effects, and Burkholderia as Important Bacteria in Multipartnered Symbioses. *Microb. Ecol.* **69**, 914–921 https://doi.org/10.1007/s00248-015-0574-y (2015).
62. Tan, Y. *et al.* Diversity and composition of rhizospheric soil and root endogenous bacteria in Panax notoginseng during continuous cropping practices. *Journal of Basic Microbiology.* **57**, 337–344 https://doi.org/10.1002/jobm.201600464 (2017).
63. Lespinet, O., Toju, H., Tanabe, A. S., Yamamoto, S. & Sato, H. High-Coverage ITS Primers for the DNA-Based Identification of Ascomycetes and Basidiomycetes in Environmental Samples. *Plos One.* **7**, e40863 https://doi.org/10.1371/journal.pone.0040863 (2012).
64. Wessels, H. H. *et al.* Massively parallel Cas13 screens reveal principles for guide RNA design. *Nat. Biotechnol.* **38**, 722–727 https://doi.org/10.1038/s41587-020-0456-9 (2020).
65. Quast, C. *et al.* The SILVA ribosomal RNA gene database project: improved data processing and web-based tools. *Nucleic Acids Res.* **41**, D590–D596 https://doi.org/10.1093/nar/gks1219 (2012).
66. Yilmaz, P. *et al.* The SILVA and "All-species Living Tree Project (LTP)" taxonomic frameworks. *Nucleic Acids Res.* **42**, D643–D648 https://doi.org/10.1093/nar/gkt1209 (2013).
67. Abarenkov, K. *et al.* (eds) et al.(ed Community UNITE) (UNITE Community, 2020).
68. Gentleman, R., Hornik, K. & Parmigiani, G. ggplot2: elegant graphics for data analysis (2nd ed.) (Springer, 2017).
69. Edgar, R. C. MUSCLE: multiple sequence alignment with high accuracy and high throughput. *Nucleic Acids Res.* **32**, 1792–1797 https://doi.org/10.1093/nar/gkh340 (2004).
70. Price, M. N., Dehal, P. S. & Arkin, A. P. FastTree 2–approximately maximum-likelihood trees for large alignments. *Plos One.* **5**, e9490 https://doi.org/10.1371/journal.pone.0009490 (2010).
71. Parks, D. H., Tyson, G. W., Hugenholtz, P. & Beiko, R. G. STAMP: statistical analysis of taxonomic and functional profiles. *Bioinformatics.* **30**, 3123–3124 https://doi.org/10.1093/bioinformatics/btu494 (2014).
72. Faust, K. & Raes, J. CoNet app: inference of biological association networks using Cytoscape. *F1000Res* **5**, 1519, https://doi.org/10.12688/f1000research.9050.2 (2016).
73. Su, G., Morris, J. H., Demchak, B. & Bader, G. D. Biological network exploration with Cytoscape 3. *Curr Protoc Bioinformatics.* **47**, 81311–81324 https://doi.org/10.1002/0471250953.bi0813s47 (2014).
74. Weiss, S. *et al.* Correlation detection strategies in microbial data sets vary widely in sensitivity and precision. *The ISME Journal.* **10**, 1669–1681 https://doi.org/10.1038/ismej.2015.235 (2016).

Figures

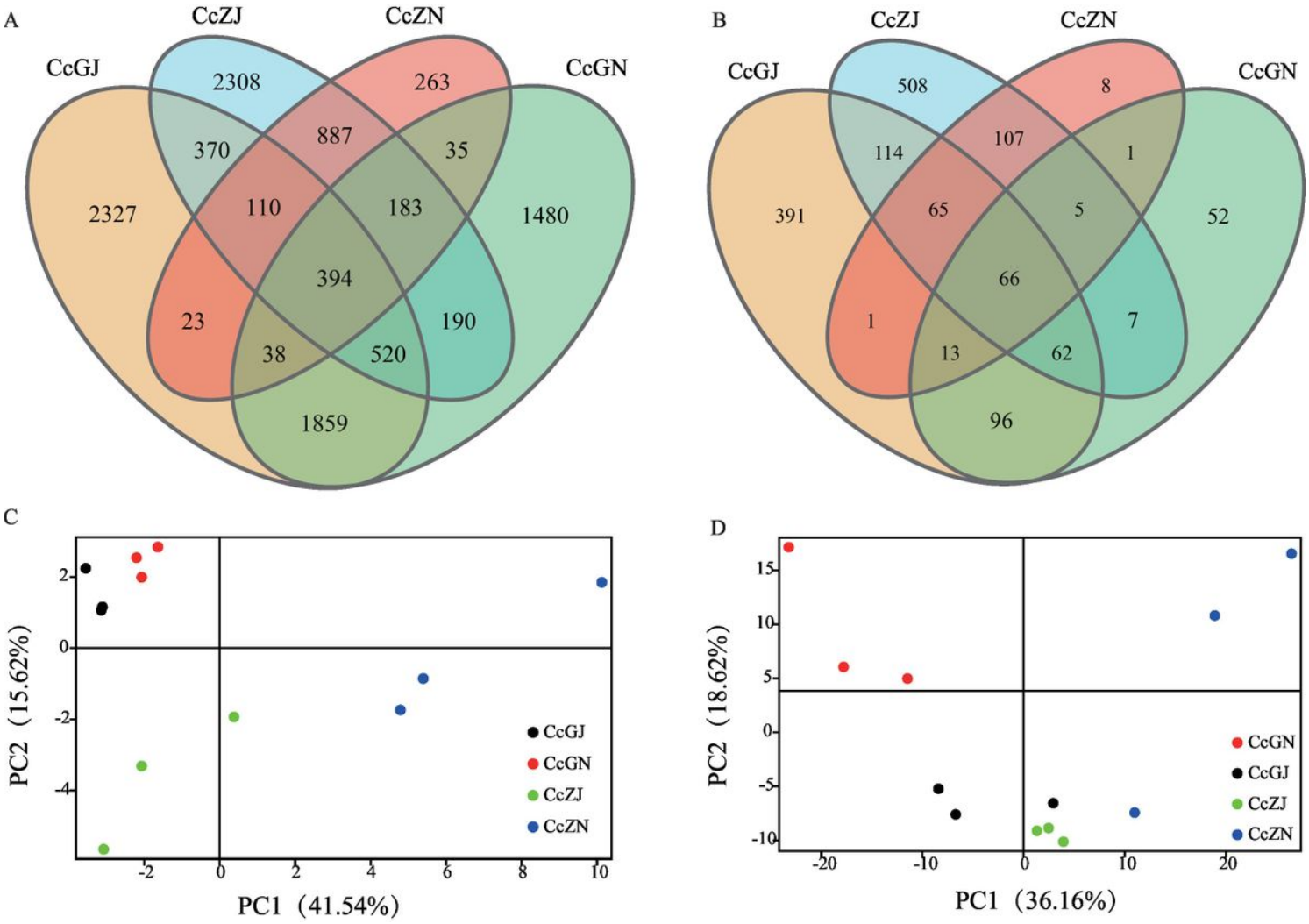

Figure 1

OUT variance analysis of microbial in the rhizosphere and the endospheree of normal and diseased Coptis chinensis. A: Venn diagram of bacteria; B: Venn diagram of fungi; C: PCA analysis of bacteria community; D: PCA analysis of fungi community.

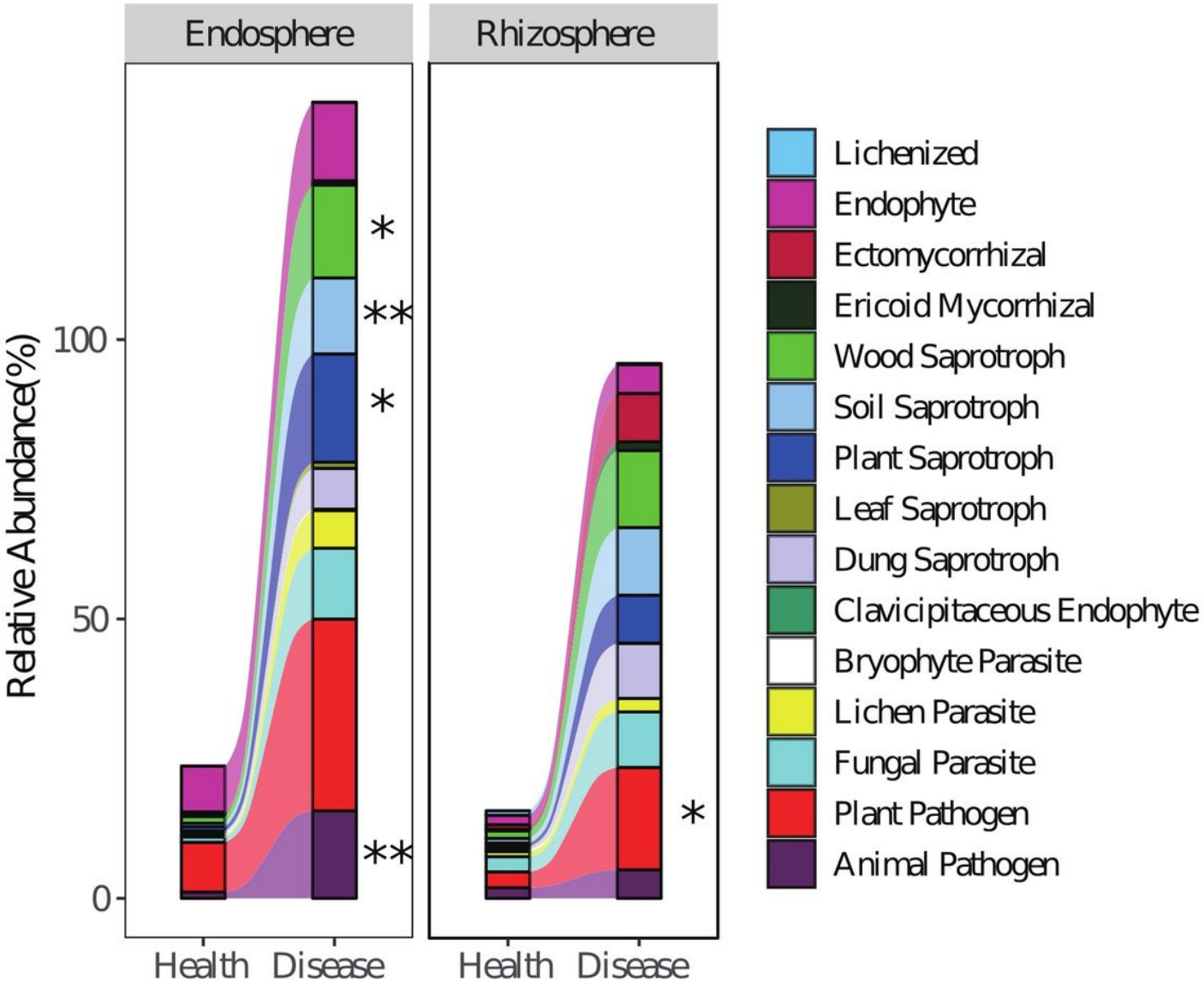

Figure 2

Stacked shock map of function group distribution of fungus community in the rhizosphere and the endosphere of diseased and normal C. chinensis. *:0.01 <P≤ 0.05; **: P ≤ 0.01；Welch\'s t test；

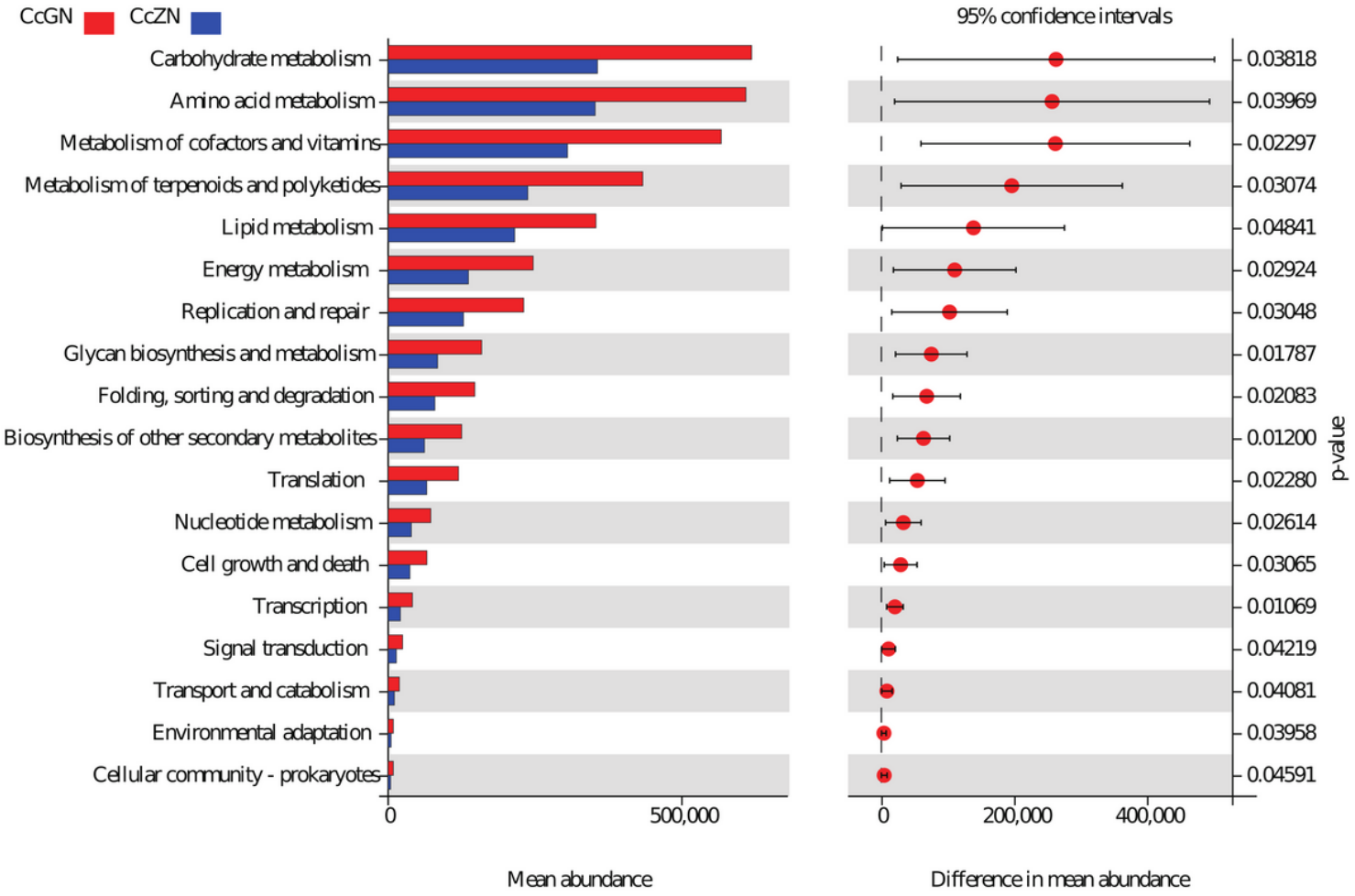

Figure 3

Prediction and analysis of significant differences between bacteria community distribution in the endosphere of normal and diseased C. chinensis. The pathways were predicted based on 16S sequences. The predicted metabolic pathways belonging to ‘Organismal Systems’ and ‘Human Diseases’ on KEGG database were discarded.

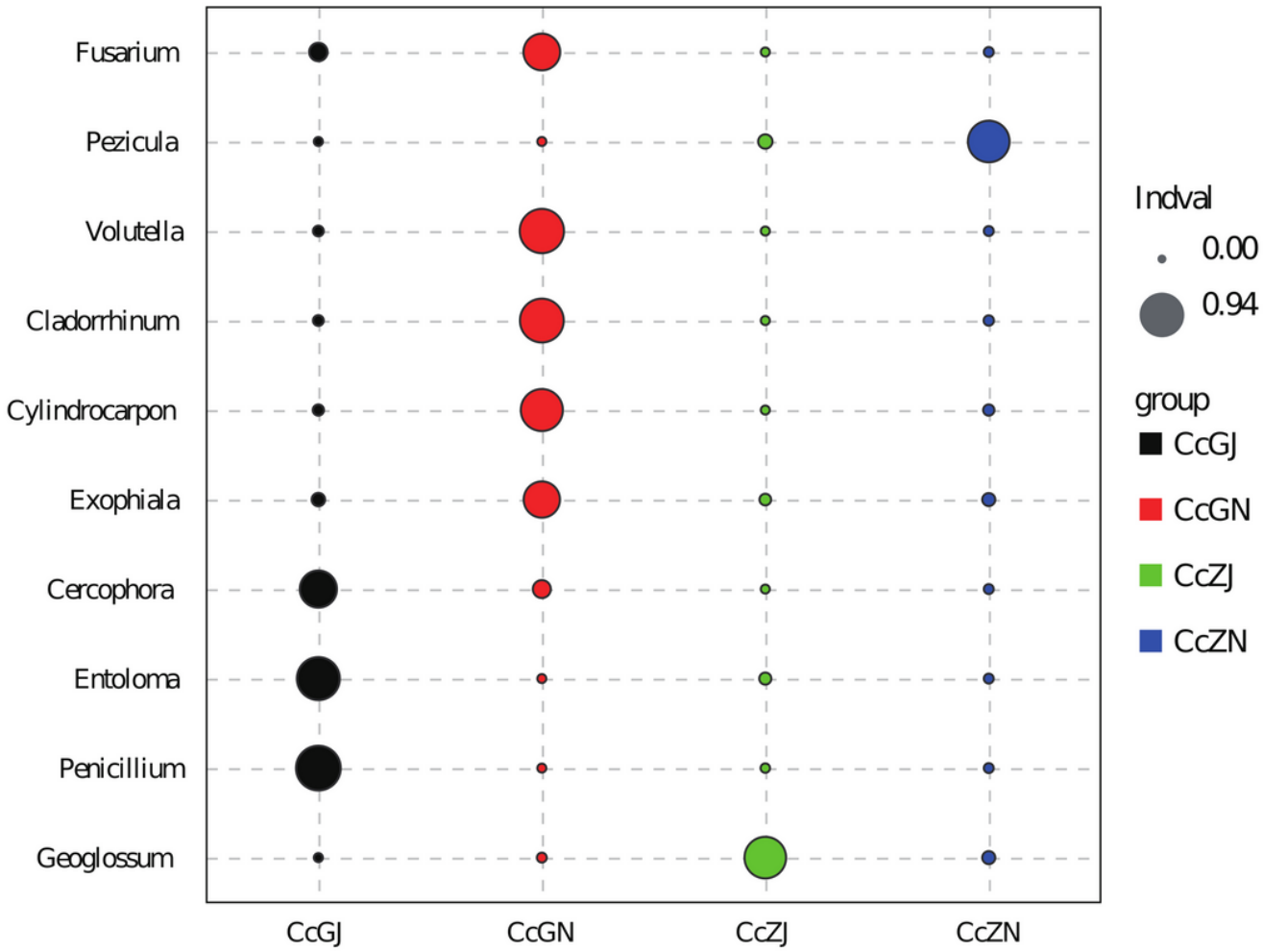

Figure 4

Analysis of indicator species of fungi in the rhizosphere and the endosphere of healthy and diseased C. chinensis.

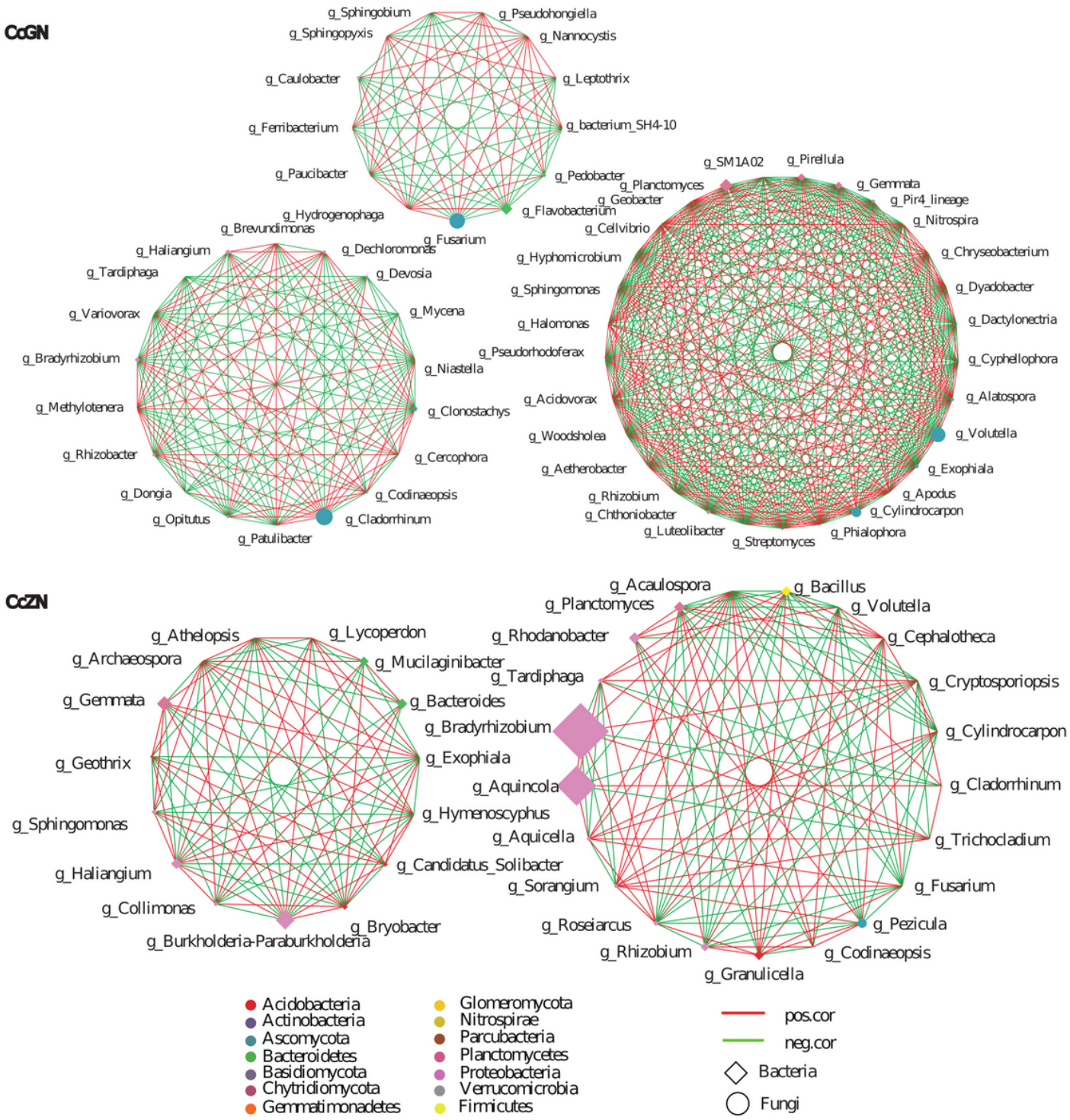

Figure 5

Microbial network in the endosphere of health and diseased C. chinensis

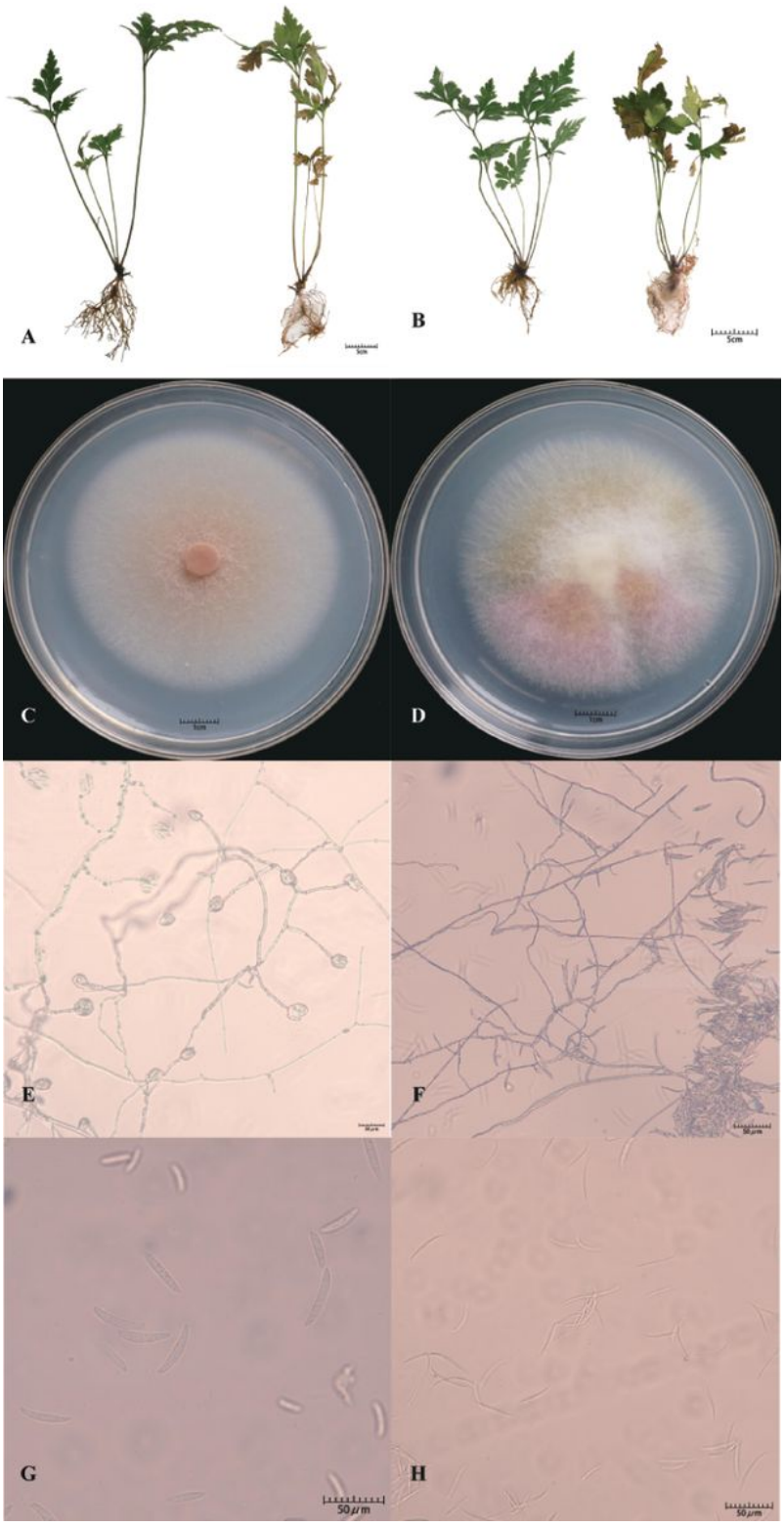

Figure 6

Pathogenicity determination and morphological identification of pathogenic fungi. A, B: Pathogenicity determination of H1 and H2; C, D: Colony characteristics on PDA of H1 and H2; E, F: Microconidia in situ on PDA of H1 and H2; G, H: Macroconidia in situ on PDA of H1 and H2.

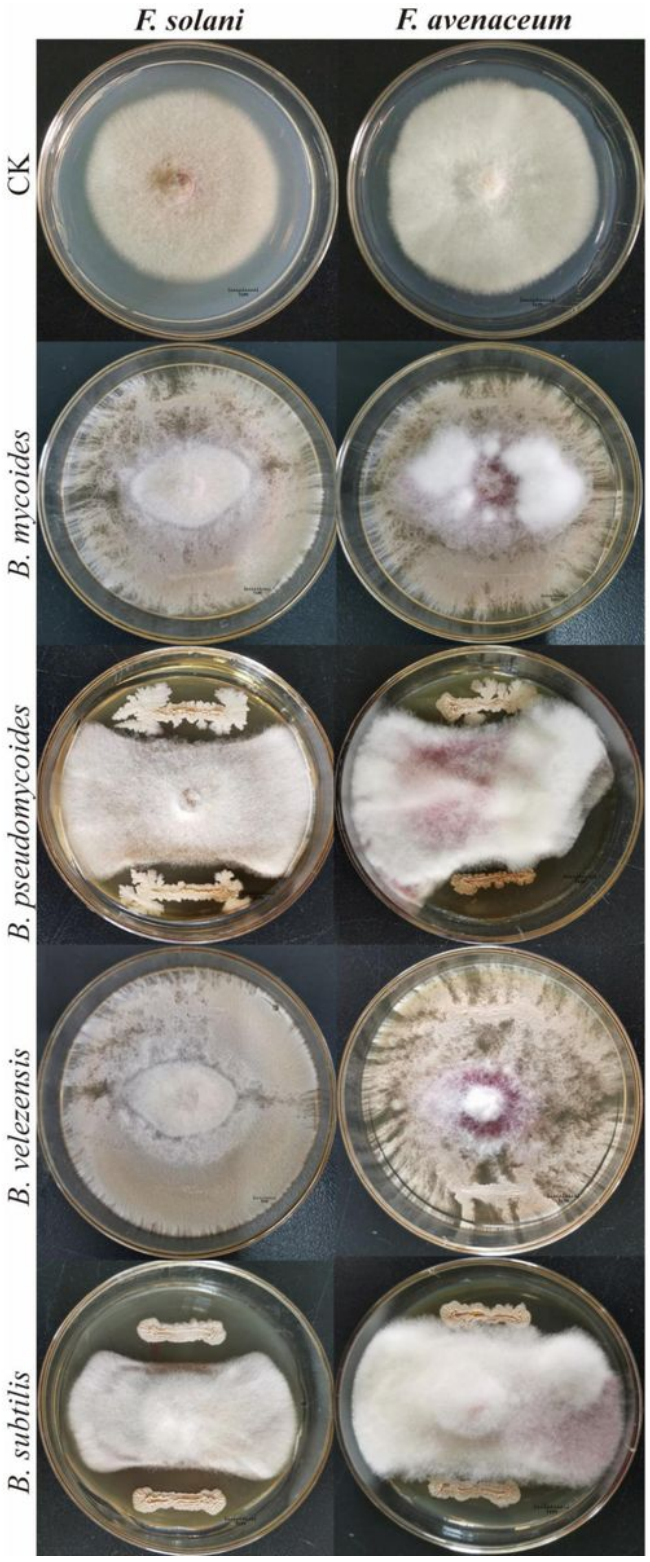

Figure 7

Bacteria with antagonistic activity against root rot pathogens of C. chinensis by the dual culture method

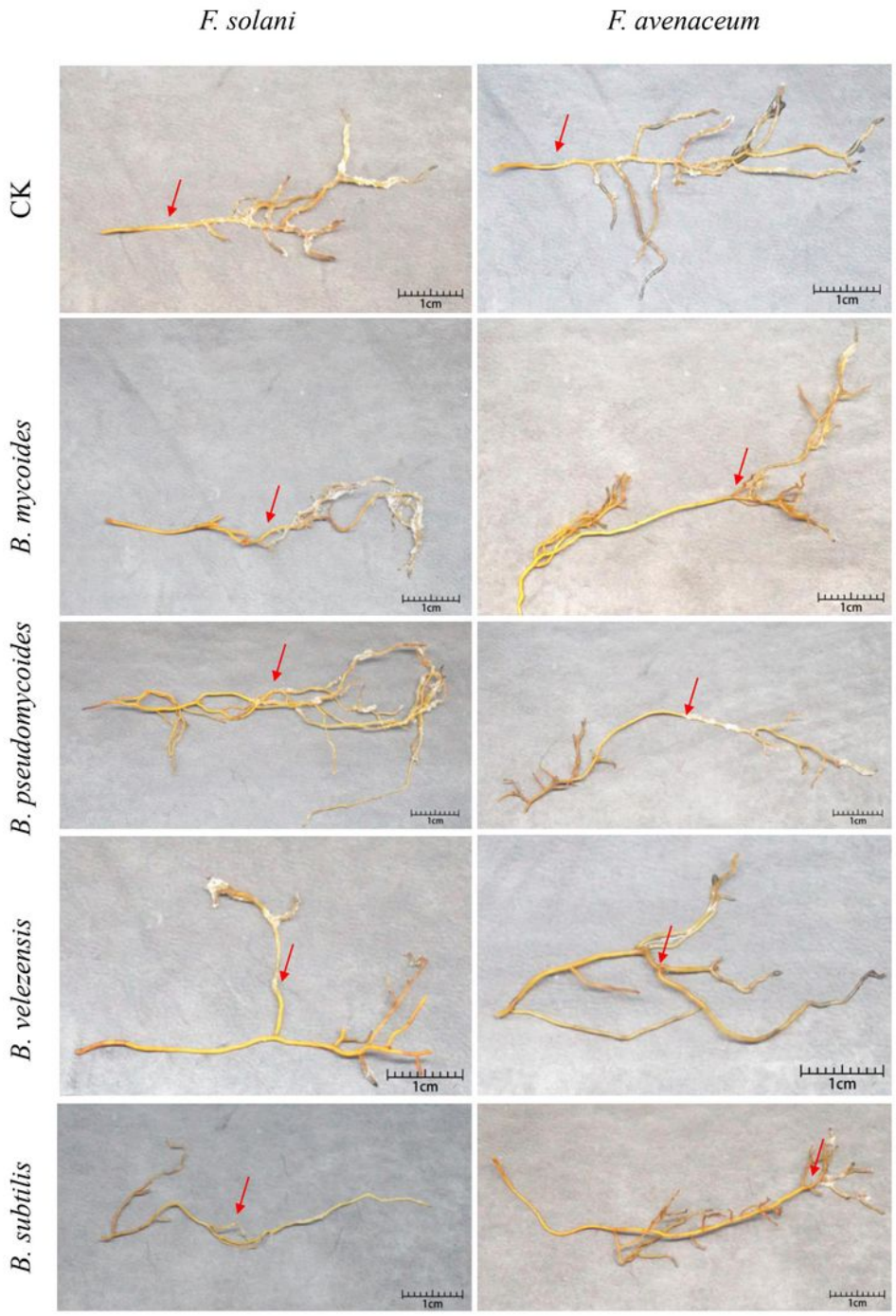

Figure 8

Bacteria with antagonistic activity against root rot pathogens of C. chinensis in detached root. The red arrow indicates the growth inhibition site of pathogen infection.

Supplementary Files

This is a list of supplementary files associated with this preprint. Click to download.

- SupplementaryMaterials.docx